Summer 8-31-2020

Theoretical Foundation of Solution Dehydration in Porous Media: Effect of Microstructure and Solute Interactions

FERNANDA SULANTAY VARGAS
fernandasulantay@uconn.edu

Theoretical Foundation of Solution Dehydration in Porous Media: Effect of Microstructure and Solute Interactions

Fernanda Sulantay Vargas

Thesis Supervisor/Honor's Advisor: Leslie Shor

Department of Chemical and Biomolecular Engineering

University of Connecticut

Table of Contents

Abstract

Retention and evaporation of water have important implications in many natural and industrial settings. Here we focus on the effect of solute components (salts) as well as system geometry on evaporation rate of water. The study of multicomponent solutions with phase changes is challenging topic because of the complex and inter-connected physical phenomena that govern its dynamics. In the present work we review the theory of water evaporation and simulate evaporation of water as a function of composition and geometry for both droplets and bulk-scale (slit-like) systems. For droplets, we studied levitated droplets and droplets over hydrophobic and hydrophilic surfaces. The Maxwell approach, the d^2 law, the Constant Contact Area mode (CCR) and Constant Contact Angle mode (CCA), the Hertz-Knudsen (HK) relation, and Fick's law of diffusion were examined. Here, we find the droplet radius influences the solution's evaporation time for both water and aqueous salt solutions at the droplet level. Larger droplets exhibit longer drying times, and the presence of salt also increases drying time. Evaporation was modeled at the bulk scale and compared to published results of drying times for aqueous solutions. We find there is a 13% discrepancy between the measured and simulated results, likely accounting for external mass transport limitations in the experimental system.

Introduction

Retention and loss of moisture in soil has a profound effect on agricultural production and the productivity of terrestrial ecosystems. The soil water content connects microbial communities (found around plants) and also controls their access to substrates. Since bacteria secrete extracellular polymeric substances (EPS), they also directly influence soil's moisture conditions [1]. Microbial EPS production reduces water evaporation and increases residual saturation in porous media. At the pore scale, both geometry and salt content have impact both the production of EPS and the retention of soil moisture. It is necessary to better understand how water evaporation is affected by system geometry and salt content with and without EPS to better develop biotechnology for more sustainable agro-ecosystems. In the present work we focus on theory and simulation of water evaporation in different geometries and with and without solutes.

Droplet evaporation is a complex diffusion phenomenon in which momentum, energy, and species transports are considered for modeling the system[2]. Droplet evaporation is controlled by the physical properties of the liquid phase (molecular weight, density, diffusion coefficient in air, and the heat of evaporation). There is no heat applied to our system, therefore, the droplet evaporation is driven by the concentration gradient of water between the droplet surface and the ambient. The vapor concentration around the droplet is assumed to be quasi-steady because the time scale in which a droplet of micro-size is diffused is much smaller than the total evaporation time [3,4]. The Maxwell approach is used to model levitated water droplets and the d^2 law is used to model levitated salt aqueous solution droplets. For droplet over surfaces, the drying times at different contact angles were calculated at a droplet scale using two evaporation modes based on experimental observations that are related to the surface properties: Constant Contact Area mode (CCR) and Constant Contact Angle mode (CCA) by Picknett and Bexon. Hydrophobic surfaces

are associated with the CCA mode and hydrophilic surfaces are associated with the CCR mode. At a larger scale, the Hertz-Knudsen (HK) relation is used to model water evaporating. And Fick's law of diffusion is used to model salt aqueous solutions evaporating.

Theory

Table 1. Methods used to evaluate solution's evaporation.

Solution Type	Droplet Scale		Bulk Scale
One-component Solution (DI Water)	Maxwell Approach	CCA and CCR modes	Hertz-Knudsen (HK) relation
Two-component Solution (Water-Salt)	The d^2 law	CCA and CCR modes	Fick's Law of Diffusion

Table 1 summarizes the different methods used to calculate the drying times for one and two component solutions at both the droplet and bulk scale.

Droplet Scale

One-Component Solution (DI Water)

Maxwell approach

In 1877, James Clerk Maxwell proposed a model for the evaporation rate of a water droplet by deriving the classic relationship diffusion-driven evaporation of the aerosol droplet[5]. Starting from a mass flux equation integrated over the droplet surface:

$$\dot{m} = \int_S \left(-\rho D_{vap} \nabla Y + \rho u Y\right) * n dS$$

Then by applying the following assumptions [2]:

- Uniform and constant droplet temperature
- A stationary gas phase
- The convective term that arises from the radius regression velocity (Stefan flow) is neglected

- The concentration gradient over an appropriate distance Δh from the surface where concentration of the vapor vanishes is linearized
- Gas phase is quasi-steady and spherically symmetric
- Properties are constant and appropriately averaged

The following expression, that applies to droplets bigger than 1um, can be recovered[5]:

$$\dot{m} = 4\pi r_s^2 \frac{D_{vap} M_{w,vap}}{RT_l} \frac{P^{sat}(T_l)}{\Delta h}$$

where:
$\dot{m}$ = mass rate $[\frac{kg}{s}]$
r_s = radius of the droplet [m]
D_{vap} = mass diffusivity $[\frac{m^2}{s}]$
$M_{w,vap}$ = molecular weight $[\frac{kg}{mol}]$
R = gas constant = 8.314 $\frac{kg*m^2}{\frac{kg}{mol}s^2}$
T = Temperature [K]
Δh = distance in which the mass transport is taking place [m]

CCA and CCR modes (Surface control)

Picknett and Bexon [4] were pioneers working on droplet evaporation placed on a substrate in still air. They presented two evaporation modes of droplet evaporation resting on a smooth and homogenous surface: constant contact area mode (CCR), and constant contact angle mode (CCA). They assumed a spherical droplet and they provided a theoretical solution of contact radius in CCA stage and a numerically simulated one for the CCR-mode. The general mechanism consists of the droplet on the stage CCR (Constant Contact Radius) mode at first. Then there is a short transition called the stick-slip behavior, in which the contact radius decreases while the contact angle increases. After that transition, the droplet evaporates in the CCA (Constant Contact Angle) mode. When the stage is over, both the contact radius and the contact angle are changed, and this stage is called mixed-mode evaporation.

CCA **CCR**

$$\frac{dW}{dt} = -kE\left(\frac{C}{r}\right)\frac{W^{\frac{1}{3}}}{2\rho^{\frac{1}{3}}} \qquad \frac{dW}{dt} = -\frac{kEW_0^{\frac{1}{3}}sin\theta_0}{\pi\rho^{\frac{1}{3}}}$$

They derived these equations based on the diffusive concentration field around the droplet and its similarity to the electrostatic potential field of a body with same size and shape as the droplet. This approach, however, made it difficult to find an exact solution to the sessile droplet evaporation problems due to the experiment specific nature of the approximations and simplifications in the model. In the diffusion-only evaporation model, the evaporation flux J(r) on the surface of the droplet in a toroidal coordinate system[6] is:

$$J(r) = \frac{D(C_s - C_\infty)}{R_c}\left[\frac{1}{2}sin\theta + \sqrt{2}(cosh\alpha + cos\theta)^{\frac{3}{2}}\int_0^\infty \frac{cosh\theta\tau}{cosh\pi\tau}\tanh[(\pi-\theta)\tau]\, P_{-\frac{1}{2}+I\tau}(cosh\alpha)\tau\, d\tau\right]$$

Where:
D = coefficient of vapor diffusion $[\frac{m^2}{s}]$
C_s = saturated vapor concentration on the droplet surface $[\frac{mol}{m^3}]$
C_∞= concentration of water vapor at infinity $[\frac{mol}{m^3}]$
R_c= contact radius of the droplet [m]
θ = contact angle of the droplet
$\tau = \frac{t}{t_f}$ [dimensionless]
t = time [s]
$t_f = \frac{\pi\rho R_i^2\theta_i}{16D(C_s - C_\infty)}$ [s]

r = radial coordinate at the baseline of the droplet such that r = R_c at the contact line.
α and β are toroidal coordinates and are related to the height (h), contact radius R_c, and contact angle θ of the droplet:

$$\cosh\alpha = \frac{\sin\theta}{h/R_c} - \cos\theta$$

Popov found the nonuniformity of the evaporation flux around the surface of the droplet to be a problem. Popov derived an analytical diffusion model for quasi-steady natural evaporation of a droplet [3]. He proposed a closed-form expression obtained by integrating the evaporating flux over the droplet surface area. The expression is based on the contact angle (valid for all the range of contact angles) and the contact radius Rc.

The rate of mass loss is:

$$\frac{dM}{dt} = \rho_L \frac{dV}{dt} = -\pi R_c D(C_s - C_\infty) f(\theta)$$

Where:

$f(\theta) = \frac{sin\theta}{1+cos\theta} + 4\int_0^\infty \frac{1+\cosh 2\theta\tau}{\sinh 2\pi\tau} \tanh[(\pi-\theta)\tau] d\tau$, is the functional variation of contact angle evaluated using a numerical integration scheme in MATLAB.

M = droplet mass [kg]

ρ_L = liquid density $[\frac{kg}{m^3}]$

V = droplet volume $[m^3]$

Using the spherical-cap assumption, which requires gravity to be negligible [7], we obtain:

$$M = \frac{\pi \rho_L R_c^3}{3g(\theta)}$$

Where:

$R_c = (\frac{3}{\pi} V g(\theta))^{\frac{1}{3}}$

$g(\theta) = \frac{sin^3\theta}{(1-cos\theta)^2(2+cos\theta)}$

With the assumption that the droplet's surface is ideally smooth with no irregularities and that the evaporation occurs at a constant angle (similar to drops suspended in air), the transient volume (temporary volume) is [3]:

$$V^{\frac{2}{3}} = V_i^{\frac{2}{3}} - \frac{2\pi D(C_s - C_\infty)}{3\rho_L}\left(\frac{3}{\pi}\right)^{\frac{1}{3}} g(\theta)^{\frac{1}{3}} f(\theta) t$$

Complete evaporation is calculated by:

$$t_{tot} = \frac{\rho_L}{2D(C_s - C_\infty)} (\frac{3V_i}{\pi})^{\frac{2}{3}} \frac{1}{\left(g(\theta)\right)^{\frac{1}{3}} f(\theta)} = kV_i^{\frac{2}{3}}$$

Where:

$$k = \frac{\rho_L}{2D(C_s - C_\infty)} \left(\frac{3}{\pi}\right)^{\frac{2}{3}} \frac{1}{\left(g(\theta)\right)^{\frac{1}{3}} f(\theta)}$$

Two-Component Solution (Water-Salt)

The d^2 law

To calculate the mass transport of a water droplet, we can use the d^2 law. The d^2 law considers the effect of the vapor pressure depression on the basis of Raoult's law and it assumes a system with constant salt concentration. The d^2 law's equation[8] is:

$$(\frac{d}{d_0})^2 = 1 - \frac{8DM}{\rho R} \left(\frac{d}{d_0}\right)^2 \frac{t}{d_0^2}$$

Where:

D = diffusion coefficient [$\frac{m^2}{s}$]
M = molecular weight [kg/mol]
ρ = density [$\frac{kg}{m^3}$]
R = gas constant = 8.3143x10^3 [$\frac{Nm}{kg\ mol\ K}$]
P = vapor pressure [Pa]
T = temperature [K]
RH = relative humidity
t = time [s]
d_0 = initial equivalent diameter of the droplet [m]
The subscript "sur" represents the droplet surface and ∞ represents the ambient gas.

In ideal solutions containing nonvolatile solutes, the equilibrium vapor pressure of water depends on its mole fraction in solution. Since the water is evaporating, the mole fraction will change

over time. Thus, for multi-component droplet with vapor pressure depression, Combe and Donaldson[9] incorporated the solute mole fraction (Z_s) and the van't Hoff factor (i) :

$$(\frac{d}{d_0})^2 = 1 - \frac{8DM}{\rho R}(\frac{P_{sur}(1 - iZ_s)}{T_{sur}} - \frac{P_\infty}{T_\infty}\frac{RH}{100})\frac{t}{d_0^2}$$

Where:

Z_s = solute molar fraction [dimensionless]
i = van't Hoff factor [dimensionless]

Mayurama and Hasegawa [8], performed an experimental investigation of the evaporation process of a salt solution droplet via acoustic levitation. Their experimental results were in partial agreement with the d^2-law when the vapor pressure depression was considered. Vapor pressure depression is the change in vapor pressure that occurs when a solute is added to a solvent. They found that the time needed for the salt to completely precipitate in the solution could be calculated with the following equation:

$$t_p = \frac{d_0^2}{\beta}$$

$$\beta = \frac{8DM}{\rho R}(\frac{P_{sur}(1 - iZ_s)}{T_{sur}} - \frac{P_\infty}{T_\infty}\frac{RH}{100})\frac{t}{d_0^2}$$

For non-ideal mixtures, Raoult's law can be used:

$$P_i = X_i * P_{i,sat} * \gamma_i$$

Where:

X_i = mole fraction [dimensionless]
γ_i = Water activity coefficient [dimensionless]
P_i = partial pressure [Pa]

CCA and CCR modes (Surface Control)

Vapor-gas convection is the prevailing factor controlling droplet evaporation when there is no droplet boiling [10]. Misyura presented different regimes of droplet evaporation: constant

contact line (radius) (CR), constant contact angle (CA), and a regime with a sliding and jumping contact line. The CA regime is represented by the following equation:

$$\frac{dm}{dt} = k_1 m^{\frac{1}{3}}$$

Where k_1 is the coefficient independent on mass.

The equation above can be manipulated to show:

$$(\frac{m}{m_0})^{\frac{2}{3}} = 1 - k_2 t;\ \frac{m}{m_0} = (1 - k_2 t)^{\frac{3}{2}}$$

The CR regime is represented by the following equation:

$$j_d = \frac{dm}{dt} = -\pi r D \Delta\rho f(\theta) = -\frac{\pi r D M (p_s - p_\infty)}{R T_s} f(\theta)$$

$$f(\theta) = 1.3 + 0.27\theta^2$$

Where:

r = droplet radius [m]
M = molar mass [kg/mol]
p_s = equilibrium vapor pressure at the interface [Pa]
ρ_∞ = vapor density of air [Pa]
D = diffusion coefficient [$\frac{m^2}{s}$]
f(θ) = function of the contact angle θ [11].

Bulk Scale

One-Component Solution (DI Water)

Hertz-Knudsen (HK) relation

The Hertz-Knudsen (HK) relation has been widely used to model water evaporating for the past 130 years because of its simplicity. However, the predictions found using the HK relation have been inconsistent with experimental results [12].

The molecular flux is found with the following equation:

$$j^{LV} = \sqrt{\frac{m}{2\pi k_B}} (\sigma_e \frac{P_s(T^L)}{\sqrt{T_l^L}} - \sigma_c \frac{P^V}{\sqrt{T_l^V}})$$

Where:

P = pressure [Pa]
T = temperature [K]
m = mass of a molecule [kg]
k_B = Boltzmann constant = 1.38064852 × 10-23 $[\frac{m^2 kg}{Ks^2}]$
The superscripts L or V denote a property of the liquid or vapor phase, respectively; while the subscript *l* indicates an interfacial property.

σ_e is the evaporation coefficient and σ_c is the condensation coefficient. These coefficients represent the fraction (0 to 1) of molecules that strike the interface and change phases. The coefficient equals 1 if all molecules that collide with the interface change phase.

Persad and Ward[12], pointed out that the evaporation and condensation coefficients have been found to vary by 3 orders of magnitude. They examined the HK relation and a modified HK relation obtained from the statistical rate theory (SRT) for the evaporation flux. They found a successful solution by incorporating a new physical concept: the coupling between the vapor and liquid phases during evaporation.

They proposed the following equations for the evaporation and condensation coefficient:

$$\sigma_e^* = \frac{P_s(T_I^L)}{P^V} \exp\left[(DOF+4)(1-\frac{T_I^V}{T_I^L})\right](\frac{T_I^V}{T_I^L})^{(DOF+4)}$$

$$\sigma_e^* = \sqrt{\frac{T_I^V}{T_I^L}} \exp\left[-(DOF+4)(1-\frac{T_I^V}{T_I^L})\right](\frac{T_I^V}{T_I^L})^{(DOF+4)}$$

Where:

DOF = Degrees Of Freedom

Two-Component Solution (Water-Salt)

Fick's Law of Diffusion

The mechanism for diffusion of gases in porous media when the pores are small in diameter is defined by the diameter of the pores[13]. The Knudsen number is needed to define which diffusion type applies to the system in question (Knudsen diffusion, molecular diffusion or a transition-region diffusion.)

The Knudsen Number equation is:

$$N_{Kn} = \frac{\lambda}{2\bar{r}}$$

Where λ is the mean free path and $\bar{r}$ is the pore radius.

The mean free path is the average distance a gas molecule travels before it collides with another gas molecule and is found with the following equation:

$$\lambda = \frac{3.2\mu}{P}\sqrt{\frac{RT}{2\pi M}}$$

Where:

λ = mean free path [m]
μ = viscosity [Pa*s]
P = pressure [N/m^2]
T = temperature [K]
M = molecular weight [kg/mol]
R = gas constant = 8.3143x10^3 [N*m/kg mol*K]

Low P gives large values of λ. For liquids, λ is so small that diffusion follows Fick's laws.

The λ of our system is intermediate size, therefore, both molecule-wall and molecule-molecule collisions are important, and the diffusion is transition-region diffusion.

The flux equation is:

$$N_A = -\frac{D_{NA}P}{RT}\frac{dx_A}{dz}$$

Where:

$D_{NA} = \frac{1}{\frac{1-\alpha x_A}{D_{BA}}+1/D_{KA}}\ [\frac{m^2}{s}]$

P = pressure [Pa]

x_A = mole fraction [dimensionless]

R = gas constant = 8.3143×10^3 [N*m/kg mol*K]

T = temperature [K]

z = distance in which the mass transport is taking place [m]

α = flux ratio factor = $1 + \frac{N_B}{N_A}$

N_i = number of moles of species i

D_{BA} = Diffusion of component B on A $[\frac{m^2}{s}]$

D_{KA} = Diffusion of component K on A $[\frac{m^2}{s}]$

At low P, the system reduces to the Knudsen equation. At high P, it reduces to the molecular diffusion equation. The water activity coefficient was used to account for deviation from ideal solutions.

Results and Discussion

System simulations were carried out at constant T = 23°C and P =1 atm. The initial liquid temperature was equal to the ambient temperature. Relative humidity was 80%. At a droplet scale, for levitated droplets, the geometry of the droplet is assumed to be spherical and we chose to illustrate the difference in evaporation flux from chamber geometry with initial droplet radius of 50 – 400 μm. At a bulk scale, the geometry considered is a group of long narrow straight channels called a "Uniform Microcapillary Array" (UMA). The surface area of each UMA channel is $40{,}000\ \mu m^2$ and the height is $35\mu m$. Simulations are performed using MATLAB 2020.

Simulation of drying times for different droplet radii are shown in Figure 1 for deionized (DI) water and for three different aqueous salt solutions. According to Figure 1, evaporation rate is quasi-constant in time only for DI water. There is a linear relationship between water droplet radius and drying time at the microscale. For this microscale geometry, the rate of change in drying time with droplet radius is approximately of 0.00065 min per each μm increase in droplet radius width. For the aqueous salt solutions, the relationship between droplet radius and evaporation time is also increasing, as with DI water. However, here the evaporation time seems to increase faster with marginal increases in channel dimension. Thus, we can conclude that the presence of salt has the greatest effect in larger channels, where edge effects are minimized.

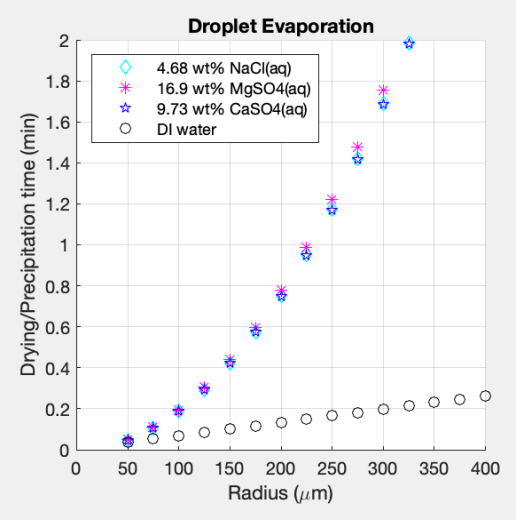

Figure 1. Drying time versus droplet radius for one-component solutions (DI water) and two-component solutions (NaCl, MgSO4, and CaSO4 aq.).

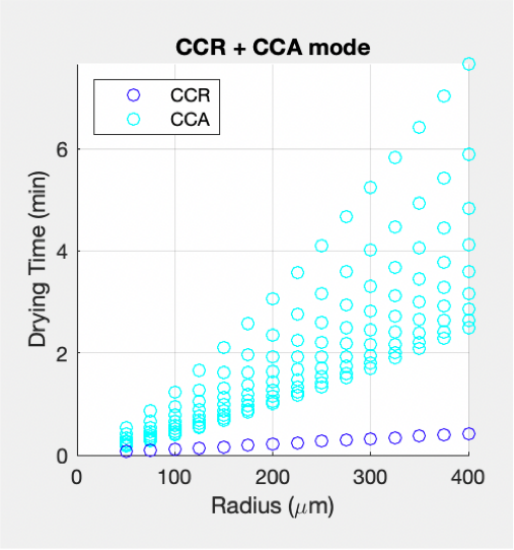

Figure 2. CCR and CCA modes at different droplet radius for one-component solution (DI Water)

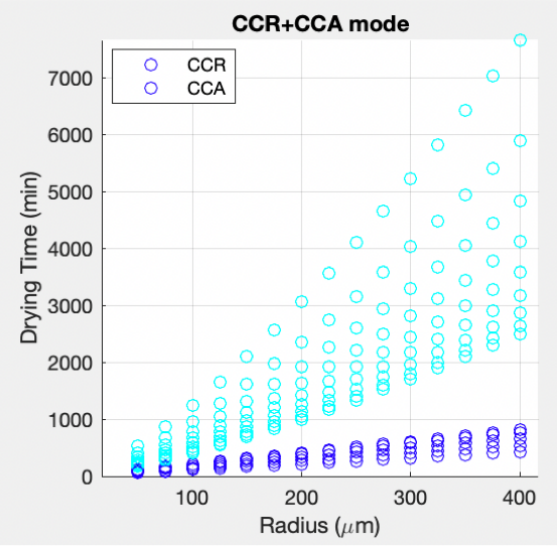

Figure 3. CCR and CCA modes at different droplet radius for two-component solution (NaCl aq. solution)

Simulated data for different droplet radius vs. drying times are shown in Figure 2 and Figure 3 for DI water solution and NaCl aqueous solution, respectively. The angle range used for the simulated data are 0 – 120 degrees every 6 degrees to test the difference in drying times

depending on the surface (hydrophobic or hydrophilic). In both solutions type, there is a linear relationship between the solution's drying time and droplet radius in the CCR mode. As droplet radius increases, the time it takes for the droplet to evaporate increases as well. In the CCA mode, the drying time and droplet radius are still directly proportional but the drying time' rate is increasing at a higher rate.

Table 2. Different drying times for DI water and NaCl aqueous solutions at angles 9° and 72°.for droplet radius of 50 μm and 400 μm.

Solution Type	**Droplet Radius**	**Angle**	**Drying Time**	
			CCR	**CCA**
DI Water Solution	50 μm	9°	7.2 s	3.9 s
		72°	0.9 s	3.8 s
	400 μm	9°	8.0 s	25 min
		72°	6.1 s	24 min
NaCl Aqueous Solution	50 μm	9°	120 min	390 min
		72°	88 min	380 min
	400 μm	9°	13 h	420 h
		72°	10 h	410 h

The drying times at angles 9° (hydrophilic surface) and 72° (hydrophobic surface) are shown in Table 2 for both DI water and NaCl aqueous solutions. In a DI water solution, when the droplet radius is held constant at 50 μm, from angle 9° to 72°, the drying time decreases from 7.2 s to 0.9 s in the CCR mode, and it decreases from 3.9 s to 3.8 s in the CCA mode. The same is observed for all angles at different radius. Thus, we conclude that the drying times are inversely proportional to the angle when the droplet is in the CCR mode as well as when it is in the CCA

mode. It is also important to note the difference in magnitude between drying times for both solutions. The drying times increase when there is salt present in water. When the droplet radius and the angle are kept constant at 50 μm and 9° respectively, the drying time in CCR mode for a DI water droplet is 7.2 s and for a NaCl aqueous droplet is 120 min. Same way, holding the same parameters constant, the drying time in CCA mode for a DI water droplet is 3.9 s and for a NaCl aqueous droplet is 390 min. The NaCl aqueous solution's drying time is around 1,000 times higher than that of DI water.

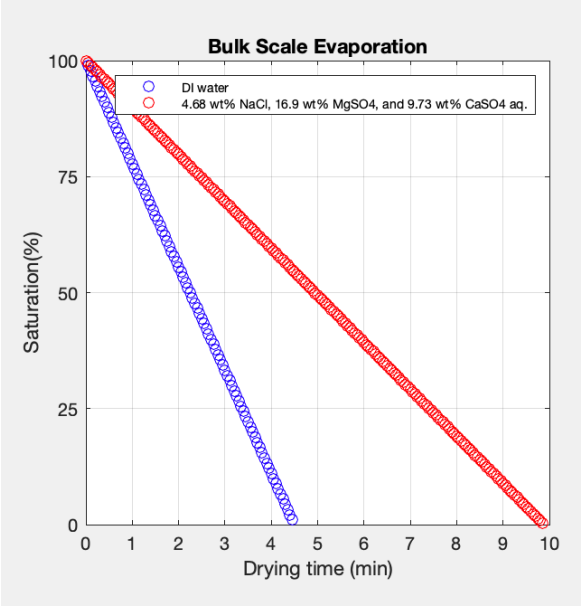

Figure 4. Drying times for one-component solutions (DI water) and two-component solutions (4.68 wt% NaCl, 16.9 wt% MgSO4, and 9.73 wt% CaSO4 aq.).

Simulated data for saturation percentage vs drying time for both DI water and salt aqueous solutions are shown in Figure 4 using the Hertz-Knudsen (HK) relation for one-component solution (DI water) and Fick's law of diffusion for the two-component solution (4.68 wt% NaCl, 16.9 wt% MgSO4, and 9.73 wt% CaSO4 aq.). According to the figure, salt aqueous solutions take longer to evaporate than the DI water solutions. This finding reinforces our conclusions drawn at the droplet scale: the presence of salt in water delays the evaporation time

of the solution. This is because the water molecules are attracted to the dissolved salt ions and it requires more energy to disrupt the attraction of water to salt and enable water molecules to evaporate.

The simulated dying time was compared with experimental results for similar-composition aqueous salt solutions evaporating in a similar settings as described in the literature[1]. The experimental drying time is 11.2 min and the simulated drying time is 9.85 min. There is a 13% discrepancy between the results. The disparity is attributed to the fact that there must be other factors that inhibit evaporation in the experimental solution that were not considered in the simulated model. For example, the RH outside the channel is 80%. Since air is not completely saturated, it drives the solution to evaporate. As the solution evaporates, the RH in the vapor phase near the air-water surface might be higher than 80%. A larger RH value decreases the evaporation's driving force. This phenomenon was not considered in the simulated model. Another possible factor could be the assumption, in the simulated model, that the salt aqueous solution is evenly mixed. The evaporation of the solution would decrease if there are more salt ions near the interface, which could be the case in the experimental model.

References

1. Guo YS, Furrer JM, Kadilak AL, et al. Bacterial extracellular polymeric substances amplify water content variability at the pore scale. *Front Environ Sci*. 2018;6(SEP). doi:10.3389/fenvs.2018.00093
2. Lupo, Giandomenico. Detailed simulations of droplet evaporation. Diss. KTH Royal Institute of Technology, 2017.
3. Dash S, Garimella S V. Droplet evaporation dynamics on a superhydrophobic surface with negligible hysteresis. *Langmuir*. 2013;29(34):10785-10795. doi:10.1021/la402784c
4. Piknett, R G, Bexon R. The evaporation of sessile or pendant drops in still air. *J Colloid Interface Sci*. Published online 1977:336-350.
5. Maxwell, James Clerk. The Scientific Papers of James Clerk Maxwell... Vol. 2. University Press, 1890.
6. Popov YO. Evaporative deposition patterns: Spatial dimensions of the deposit. *Phys Rev E - Stat Nonlinear, Soft Matter Phys*. 2005;71(3):1-17. doi:10.1103/PhysRevE.71.036313
7. Patankar NA. Transition between superhydrophobic states on rough surfaces. *Langmuir*. 2004;20(17):7097-7102. doi:10.1021/la049329e
8. Maruyama Y, Hasegawa K. Evaporation and drying kinetics of water-NaCl droplets via acoustic levitation. *RSC Adv*. 2020;10(4):1870-1877. doi:10.1039/c9ra09395h
9. Combe NA, Donaldson DJ. Water Evaporation from Acoustically Levitated Aqueous Solution Droplets. *J Phys Chem A*. 2017;121(38):7197-7204. doi:10.1021/acs.jpca.7b08050
10. Misyura SY. Evaporation of a sessile water drop and a drop of aqueous salt solution. *Sci Rep*. 2017;7(1):1-11. doi:10.1038/s41598-017-15175-1

11. Hu H, Larson RG. Evaporation of a sessile droplet on a substrate. *J Phys Chem B*. 2002;106(6):1334-1344. doi:10.1021/jp0118322

12. Persad AH, Ward CA. Expressions for the Evaporation and Condensation Coefficients in the Hertz-Knudsen Relation. *Chem Rev*. 2016;116(14):7727-7767. doi:10.1021/acs.chemrev.5b00511

13. Geankoplis, Christie J. Transport processes and separation process principles:(includes unit operations). Prentice Hall Professional Technical Reference, 2003.

14. Misyura SY. Contact angle and droplet evaporation on the smooth and structured wall surface in a wide range of droplet diameters. *Appl Therm Eng*. 2017;113:472-480. doi:10.1016/j.applthermaleng.2016.11.072

15. Chen X, Weibel JA, Garimella S V. Water and Ethanol Droplet Wetting Transition during Evaporation on Omniphobic Surfaces. *Sci Rep*. 2015;5(June):1-11. doi:10.1038/srep17110

16. Misyura SY. Free Solution Convection at Non-Isothermal Evaporation of Aqueous Salt Solution on a Micro-Structured Wall. *Nanoscale Microscale Thermophys Eng*. 2019;23(1):48-66. doi:10.1080/15567265.2018.1551448

17. Shahidzadeh N, Schut MFL, Desarnaud J, Prat M, Bonn D. Salt stains from evaporating droplets. *Sci Rep*. 2015;5:1-9. doi:10.1038/srep10335

18. Ferron GA, Soderholm SC. Estimation of the times for evaporation of pure water droplets and for stabilization of salt solution particles. *J Aerosol Sci*. 1990;21(3):415-429. doi:10.1016/0021-8502(90)90070-E